

Absence of magnetic order in dichloro [1,2-bis (diphenylphosphino) ethane] nickel^{2+} single crystal

Shuaiqi Ma(马帅奇), Linlin An(安琳琳), Xiangde Zhu(朱相德)

Citation: Chin. Phys. B, 2021, 30 (**5**): 057501. DOI: 10.1088/1674-1056/abe233
Journal homepage: http://cpb.iphy.ac.cn; http://iopscience.iop.org/cpb

What follows is a list of articles you may be interested in

Texture analysis of ultra-high coercivity Sm_2Co_7 hot deformation magnets

Qiang Ma(马强), Meishuang Jia(贾美爽), Zhifeng Hu(胡智峰), Ming Yue(岳明), Yanli Liu(刘艳丽), Tongyun Zhao(赵同云), and Baogen Shen(沈保根)
Chin. Phys. B, 2021, 30 (**4**): 047505. DOI: 10.1088/1674-1056/abe2fc

Exact soliton solutions in anisotropic ferromagnetic wires with Dzyaloshinskii-Moriya interaction

Qiu-Yan Li(李秋艳), Dun-Zhao(赵敦), and Zai-Dong Li(李再东)
Chin. Phys. B, 2021, 30 (**1**): 017504. DOI: 10.1088/1674-1056/abca26

Giant anisotropy of magnetic damping and significant in-plane uniaxial magnetic anisotropy in amorphous $Co_{40}Fe_{40}B_{20}$ films on GaAs(001)

Ji Wang(王佶), Hong-Qing Tu(涂宏庆), Jian Liang(梁健), Ya Zhai(翟亚), Ruo-Bai Liu(刘若柏), Yuan Yuan(袁源), Lin-Ao Huang(黄林傲), Tian-Yu Liu(刘天宇), Bo Liu(刘波)†, Hao Meng(孟皓), Biao You(游彪), Wei Zhang(张维), Yong-Bing Xu(徐永兵), and Jun Du(杜军)‡
Chin. Phys. B, 2020, 29 (**10**): 107503. DOI: 10.1088/1674-1056/abad1d

Role of the spin anisotropy of the interchain interaction in weakly coupled antiferromagnetic Heisenberg chains

Yuchen Fan(樊宇辰), Rong Yu(俞榕)
Chin. Phys. B, 2020, 29 (**5**): 057505. DOI: 10.1088/1674-1056/ab820b

Dynamical anisotropic magnetoelectric effects at ferroelectric/ferromagnetic insulator interfaces

Yaojin Li(李耀进), Vladimir Koval, Chenglong Jia(贾成龙)
Chin. Phys. B, 2019, 28 (**9**): 097501. DOI: 10.1088/1674-1056/ab37f7

Absence of magnetic order in dichloro [1,2-bis (diphenylphosphino) ethane] nickel^{2+} single crystal*

Shuaiqi Ma(马帅奇)[1,3], Linlin An(安琳琳)[2,3], and Xiangde Zhu(朱相德)[3,†]

[1] *Institute of Physical Science and Information Technology, Anhui University, Hefei* 230601, *China*
[2] *School of Electronic Science and Applied Physics, Hefei University of Technology, Hefei* 230009, *China*
[3] *Anhui Province Key Laboratory of Condensed Matter Physics at Extreme Conditions, High Magnetic Field Laboratory, Chinese Academy of Sciences, Hefei* 230031, *China*

(Received 7 January 2021; revised manuscript received 26 January 2021; accepted manuscript online 2 February 2021)

Dichloro [1,2-bis (diphenylphosphino) ethane] nickel^{2+} ($NiCl_2$(dppe)) is an organic compound containing $C_{26}H_{24}P_2$(dppe) molecules and Cl^-, Ni^{2+} ions. The large-size $NiCl_2$(dppe) single crystals with longest dimension of 4 mm were grown by the method of slow evaporation of organic solution. Single crystal x-ray diffraction spectrum indicates that the single crystal is of high quality. Magnetization results of the $NiCl_2$(dppe) single crystals show an anisotropic paramagnetism behavior and diamagnetic background, which come from Ni^{2+} ions and benzene ring, respectively. However, according to the specific heat results with temperature down to 0.1 K and magnetic field up to 14 T, no expected field-induced quantum phase transition was observed in $NiCl_2$(dppe) single crystals.

Keywords: anisotropic, paramagnetic, single crystal, ultra low temperature, specific heat

PACS: 75.30.Gw, 78.30.Jw, 65.40.Ba **DOI:** 10.1088/1674-1056/abe233

1. Introduction

Bose and Einstein proposed that the boson obeys the Boson–Einstein distribution and they predicted the Boson–Einstein condensate (BEC) in 1924.[1,2] The so-called Bose–Einstein condensate is that the bosons condense into a macroscopic quantum state as their temperature (T) approaches to the absolute zero. The Bose–Einstein condensate is not only a very interesting macroscopic quantum phenomenon,[3,4] but also can be used to investigate microscopic quantum phenomena.[5,6] Therefore, the research on BEC became the frontier of optical and condensed matter physics in modern physics. Many investigators used BEC to investigate quantum magnetic materials.[7,8] But for most researchers, it is too harsh to realize the BEC of ultra-cold atoms by optical method.[7,8] In 1930, Bloch treated dimers in ferrimagnets as magnons, particles with integer spin and bosonic statistics.[9] In 1956, Matsubara and Matsuda established the corresponding relationship between crystal Bose gas and quantum antiferromagnet,[10] which inspired researchers to search BEC and its relative magnetic field (H)-induced magnetic quantum phase transitions in quantum magnets, such as $TlCuCl_3$, $BaCuSi_2O_6$, and $NiCl_2{\cdot}4SC(NH_2)_2$ (DTN).[8,11–14] It was also found that the transiton tempetature of BEC increases when the boson mass decreases in the quantum magnet.[7,8] Therefore, if potential candidates for BEC magnetic materials with higher critical temperature can be experimentally discovered and confirmed, BEC materials can be used to produce quantum devices, quantum switches, and quantum computation.[15]

Dichloro [1,2-bis (diphenylphosphino) ethane] nickel^{2+} ($NiCl_2$(dppe)), an analog of DTN, is another inorganic-organic hybrid compound, which is mainly composed of benzene rings, Ni^{2+} and Cl^- ions. The $NiCl_2$(dppe) solvate has been characterized by solid-state P-31 NMR spectroscopy, x-ray diffraction, infra-red, laser Raman spectroscopy, FAB mass spectroscopy, elemental analyses, and melting points.[16–21] $NiCl_2$(dppe) crystallizes in the monoclinic structure (space group $P2_1/c$), with the Ni^{2+} ions forming zig-zag chains along c-axis (shown in Fig. 1(b)).[16]

So far, there is no report on the single crystal growth, magnetism characterization, and specific heat of the $NiCl_2$(dppe). In this paper, we successfully grow large size single crystals of $NiCl_2$(dppe) with typical dimensions of 4 mm×2 mm×1 mm via the method of slow evaporation of organic solution. The crystal structure, anisotropic magnetism properties, and ultra-low temperature specific heat of the as-grown crystals are characterized.

2. Experimental details

Single crystals of $NiCl_2$(dppe) were grown by recrystallization. Because of the toxicity and volatility of the solvent, the whole processes of single crystal preparation were carried out in a fumehood. First, $NiCl_2$(dppe) powder was dissolved in a mixture of dichloromethane and ethyl acetate or dissolved

*Project supported by the National Key Research and Development Program of China (Grant No. 2017YFA0403502), the National Natural Science Foundation of China, and Youth Innovation Promotion Association of Chinese Academy of Sciences (Grant No. 2017483). A portion of this work was supported by the High Magnetic Field Laboratory of Anhui Province, China.

†Corresponding author. E-mail: xdzhu@hmfl.ac.cn

© 2021 Chinese Physical Society and IOP Publishing Ltd

in a mixture of dichloromethane and cyclohexane. Next, in order to grow large-size single crystals, organic needle filters were used to remove impurities and nuclei from the mixture. At last, the crystal growth was realized by the recrystallization of the filtered mixture in about ten-day slow evaporation of solution. The most important point of the crystal growth is that the container cannot be moved or shaken when the crystal is growing. Following the above recrystallization method, large-size single crystals of millimeter grade can be obtained. As shown in Fig. 1(c), the typical dimensions of the $NiCl_2$(dppe) single crystal are 4 mm×2 mm×1 mm. The x-ray diffraction (XRD) measurement was carried out on Rigaku TTR3 at room temperature. The magnetization (M) measurements of $NiCl_2$(dppe) single crystal were performed with magnetic property measurement system 3 (Quantum Design, MPMS3) with zero-field cooling (ZFC) process. Magnetic field dependent magnetizations in longitudinal and transverse directions were obtained respectively for several $NiCl_2$(dppe) single crystals. The ultra-low temperature specific heat measurement was carried out on a 16 T physical properties measurement system (Quantum Design, PPMS-16T) with a dilution refrigerator using the standard thermal relaxation method.

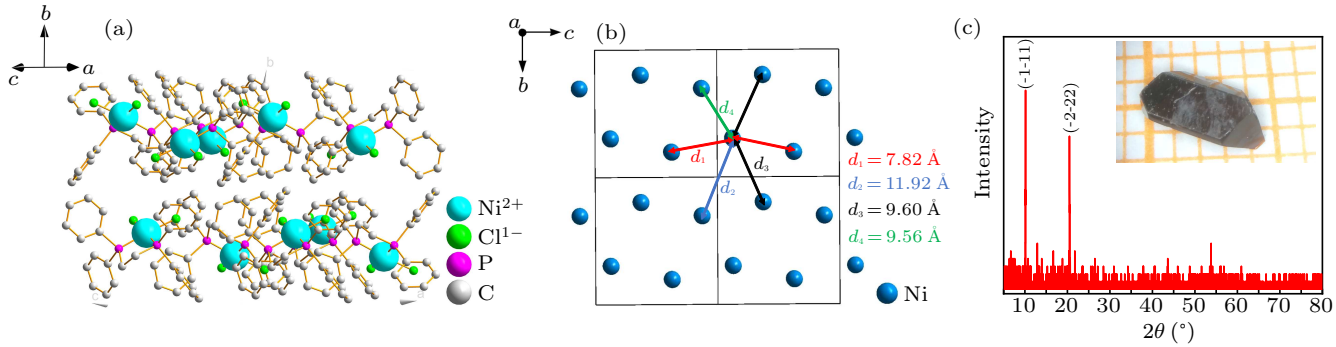


Fig. 1. (a) Crystal structure (space group $P2_1/c$) of the $NiCl_2$(dppe) single crystal. The cyan sphere represents nickel atoms, the green sphere represents chlorine atoms, the magenta sphere represents phosphorus atoms, and the silver sphere represents carbon atoms. (b) Crystal structure of Ni^{2+} of $NiCl_2$(dppe) single crystal. (c) XRD pattern of $NiCl_2$(dppe) single crystal.

3. Results and discussion

3.1. Single crystal characterization

Figure 1(a) shows the single crystal structure of $NiCl_2$(dppe) mainly consisting of benzene rings which are linked by covalent interactions. As shown in Fig. 1(b), the Ni^{2+} ions form one-dimensional zigzag chains along c-axis. The arrows with different colors represent different atomic distances, with red representing 7.82 Å, blue 11.92 Å, black 9.6 Å, and green 9.56 Å. The distance between the zigzag chains is 9.6 Å, and the distance within the chain is 7.82 Å. The nearest neighbor distances between Ni^{2+} ions are 7.82 Å, 9.56 Å, 9.6 Å, and 11.92 Å, respectively. Figure 1(c) shows the room temperature XRD pattern for the $NiCl_2$(dppe) single crystal, where only two diffraction peaks can be observed. By comparing with the previous crystal structure results,[16] the crystallographic plane of the $NiCl_2$(dppe) single crystals is (-1-11). In addition to this study, single crystals with (110) face can also obtained.

3.2. Magnetization measurements

In order to understand the magnetic properties of the $NiCl_2$(dppe) single crystal, we measured its temperature and field dependent magnetization. The results are presented in Fig. 2. Figures 2(a) and 2(b) show the temperature dependent ZFC magnetization measured under a magnetic field (H) of 0.1 T for H parallel (-1-11) plane ($H \parallel$ (-1-11)) and perpendicular to (-1-11) plane ($H \perp$ (-1-11)), respectively. In the low temperature region, the magnetization decreases exponentially, which is a classic signature of paramagnetism, while in the high temperature region it shows complete diamagnetism. Moreover, it can be observed that the magnetization at 300 K for $H \perp$ (-1-11) is about two times of that for $H \parallel$ (-1-11).

Field dependent magnetization curves of $NiCl_2$(dppe) single crystals were also measured. It is easy to observe that the magnetization at 300 K decreases with the increase of H for both $H \parallel$ (-1-11) and $H \perp$ (-1-11) in Figs. 2(c) and 2(d), and the absolute value at 7 T for $H \perp$ (-1-11) is about one time larger than that for $H \parallel$ (-1-11). Generally, as shown in Figs. 2(a)–2(d), the magnetization results for $NiCl_2$(dppe) exhibit two obvious contributions, anisotropic paramagnetic part and very strong diamagnetic part. According to Fig. 1(a), such anisotropic diamagnetism should come from benzene ring of $NiCl_2$(dppe).[22–24] Since diamagnetism is known to be temperature-independent, the magnetization curves of 300 K could be regarded as the diamagnetic background.[24] After subtraction of the diamagnetic contribution, the magnetic field dependence of magnetization at different temperatures is presented in Figs. 2(e) and 2(f).

Figures 2(e) and 2(f) show the typical anisotropic paramagnetic behavior for $H \parallel$ (-1-11) and $H \perp$ (-1-11), and the magnetization at 2 K and 7 T for $H \parallel$ (-1-11) is about three times larger than that for $H \perp$ (-1-11). The anisotropic paramagnetic behavior should come from Ni^{2+} ions of $NiCl_2$(dppe).[25] Two magnetization plateaus are observed from DTN at ultra low temperature, one is the zero plateau below the first critical magnetic field, and the other is the saturation plateau above the second critical magnetic field.[26] It is obvious that no magnetic plateau can be observed in $NiCl_2$(dppe) at 2 K.

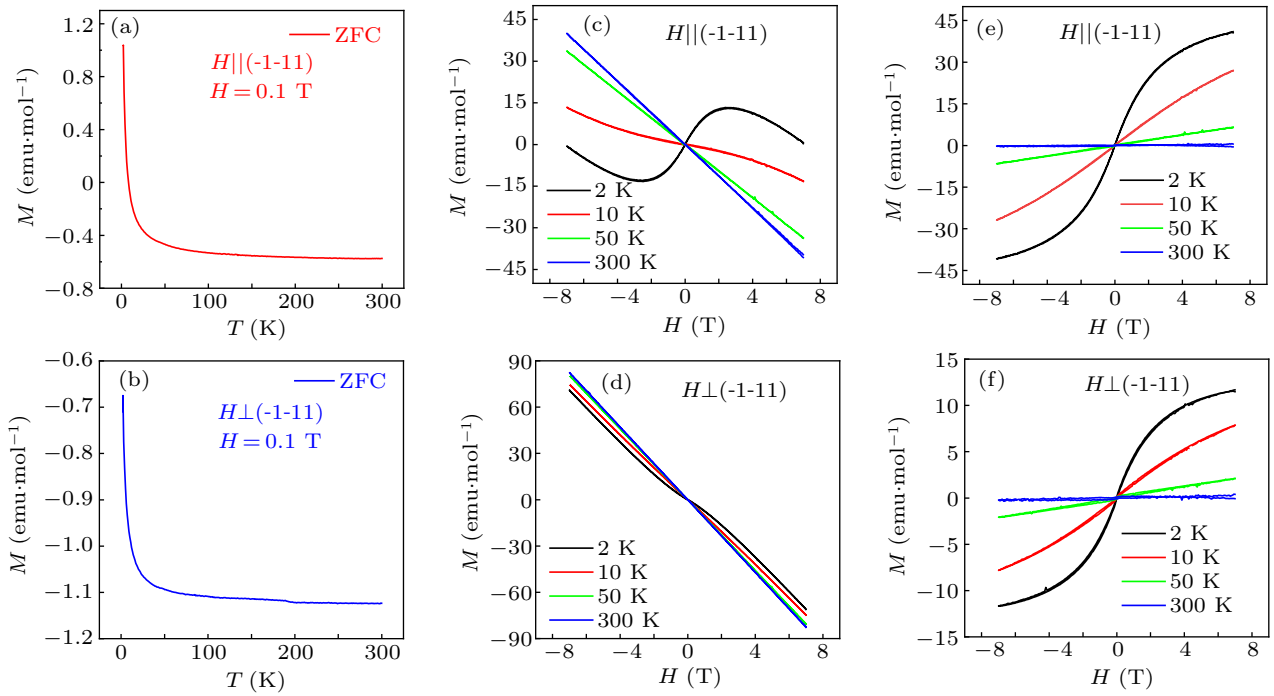


Fig. 2. (a) and (b) Temperature dependent magnetization of $NiCl_2$(dppe) single crystal with a 0.1 T magnetic field applied parallel ($H \parallel$ (-1-11)) and perpendicular ($H\perp$ (-1-11)) to the (-1-11) plane, respectively. (c) and (d) Field dependent magnetization at 2 K, 10 K, 50 K, 300 K for $H \parallel$ (-1-11) and $H\perp$ (-1-11), respectively. (e), (f) Field dependent magnetization with diamagnetizatic contributions subtracted at 2 K, 10 K, 50 K, 300 K for $H \parallel$ (-1-11) and $H\perp$ (-1-11), respectively.

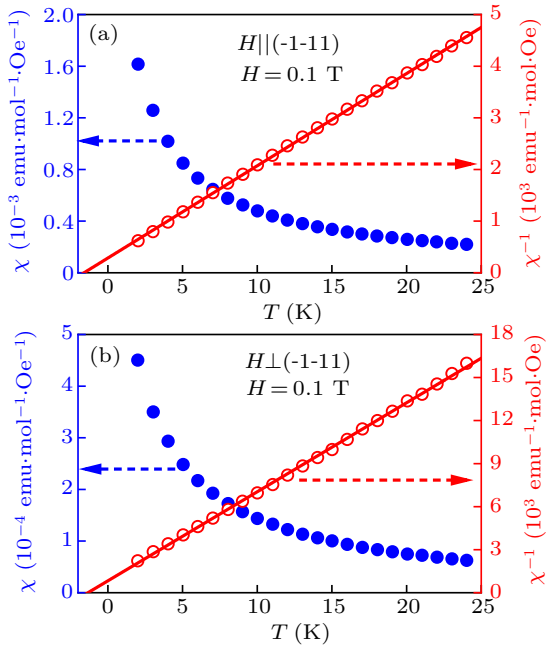


Fig. 3. (a) Blue solid circles and red hollow circles are experimental data for magnetic susceptibility of $NiCl_2$(dppe) single crystal with field of 0.1 T applied parallel to the (-1-11) plane and the inverse magnetic susceptibility H/M. The line is the fitting by the Curie–Weiss function for data from 2 K to 25 K. (b) Magnetic susceptibility versus temperature curves recorded in a field of 0.1 T and the inverse magnetic susceptibility H/M. The line is the fitting by the Curie–Weiss function for data from 2 K to 25 K.

Figures 3(a) and 3(b) show magnetic susceptibility (χ)–T and χ^{-1}–T after subtracting the diamagnetic contribution for $H \parallel$ (-1-11) and $H\perp$ (-1-11), respectively. The blue solid circles represent the experimental data of χ–T, and the red hollow circles represent the data of χ^{-1}–T, where the red line is the linear fitting of the data by using the Curie–Weiss law, $\chi = C/(T-\theta)$, here C is the Curie constant of the substance, T is the absolute temperature in units of K, and θ is the Weiss temperature of the substance in units of K.[27] By fitting the χ^{-1}–T lines between 2 K and 25 K, the C in Fig. 3(a) is 0.005618 K·emu·mol^{-1}, the absolute value of θ is 1.6011 K, the C in Fig. 3(b) is 0.001613 K·emu·mol^{-1}, and the absolute value of θ is 1.3355 K. Since the red line intersects the negative x-axis, the material is antiferromagnetic.[27] According to the values of C determined from Figs. 3(a) and 3(b), the corresponding effective magnetic moment can be calculated as 0.212 μ_B/Ni^{2+} and 0.1136 μ_B/Ni^{2+}, respectively (μ_B is the Bohr magneton). Such low effective momentum values of Ni^{2+} ions may originate from the hybridization between Ni^{2+} and its anisotropic zig-zag coordinated organic ligands.[28] We suppose that an antiferromagnetic transition may occur at much lower temperature, and that $NiCl_2$(dppe) is a potential candidate of BEC. Therefore, further magnetism investigation such as torque measurement at ultra-low temperature and high magnetic field is needed to figure out whether there is a magnetic order in the $NiCl_2$(dppe) single crystal.[29]

3.3. Specific heat measurements

The specific heat (C) at low temperature is a necessary probe to explore the existence of magnetic-field-induced quantum phase transition in single crystals of $NiCl_2$(dppe), which is measured as a function of temperature for various applied fields. Figure 4(a) presents the temperature dependent low temperature specific heat (C–T) curves under several mag-

netic fields with $H\perp$ (-1-11) for $NiCl_2$(dppe). As shown in Fig. 4(a), the specific heat increases exponentially with increasing temperature. Figure 4(b) shows the C/T–T^2 curves determined from Fig. 4(a). As shown in Fig. 4(b), the $C(T)/T$ roughly follows a linear relation of T^2. The blue dotted line in the figure is the guide line. Obviously, the C–T curve of the $NiCl_2$(dppe) single crystal is quite different from that of DTN, which exhibits a peak around the first critical magnetic field mentioned above.[14] No peak can be observed on the C–T curves for $NiCl_2$(dppe) above 0.1 K, which means no long-range magnetic order or no magnetic-field-induced quantum phase transition. As shown in Fig. 4(b), the C/T–T^2 curves for $H = 1$ T deviate from the linear relation, showing a weak hump-like feature. In addition to the electron and phonon contributions of $C/T = \gamma + \beta T^2$ (where γ and β are the free electron part coefficient and phonon part coefficient),[30] the weak hump-like feature should come from magnetism contribution of the Ni^{2+} ions. We suppose that the magnetic-field-induced quantum phase transition may occur at much lower temperature or stronger magnetic field for $NiCl_2$(dppe), which needs extremely-low temperature measurements in the future.

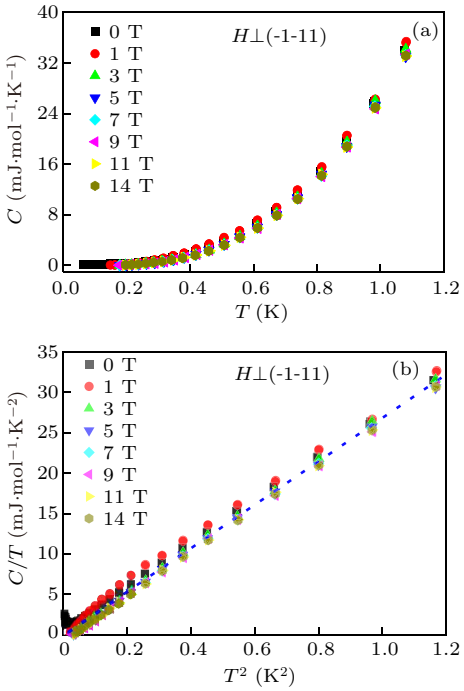


Fig. 4. (a) Specific heat C versus temperature of $NiCl_2$(dppe) for $H\perp$ (-1-11) of 0, 1, 3, 5, 7, 9, 11, and 14 T. (b) $C(T)/T$ vs. T^2 of $NiCl_2$(dppe) for $H\perp$ (-1-11) of 0, 1, 3, 5, 7, 9, 11, and 14 T.

4. Conclusions

Large-size $NiCl_2$(dppe) single crystals of high quality were grown via slow solution evaporation method at room temperature. We reported the magnetic and specific heat measurement results of $NiCl_2$(dppe) single crystals. No magnetic order was observed in $NiCl_2$(dppe) above 0.1 K, which might stem from the very weak exchange interaction caused by the large spacing of the nickel atoms. Anisotropic paramagnetic and diamagnetic contributions in $NiCl_2$(dppe) single crystal originated from Ni^{2+} ions and benzene ring, respectively. No magnetic field-induced quantum phase transition was observed in specific heat measurement above 0.1 K.

Acknowledgments

We thank professor Xiang Wu for advice on solution evaporation method. We thank Yongliang Qin and Langsheng Lin for magnetization measurements. We thank Yuyan Han for heat capacity measurements. We thank Jun Zhao and Fanying Meng for XRD measurements.

References

[1] Einstein A 1924 *Sitzber Preuss Akad* 261
[2] Bose 1924 *Z. Phys.* **26** 178
[3] Lai C W, Kim N Y, Utsunomiya S, Roumpos G, Deng H, Fraser M D, Byrnes T, Recher P, Kumada N, Fujisawa T and Yamamoto Y 2007 *Nature* **450** 529
[4] Plumhof J D, Stoferle T, Mai L J, Scherf U and Mahrt R F 2014 *Nat. Mater.* **13** 248
[5] Donley E A, Claussen N R, Cornish S L, Roberts J L, Cornell E A and Wieman C E 2001 *Nature* **412** 295
[6] Bloch I, Hansch T W and Esslinger T 2000 *Nature* **403** 166
[7] Zapf V, Jaime M and Batista C D 2014 *Rev. Mod. Phys.* **86** 563
[8] Giamarchi T, Ruegg C and Tchernyshyov O 2008 *Nat. Phys.* **4** 198
[9] Bloch F 1930 *Z. Phys.* **61** 206
[10] Matsubara T and Matsuda H 1956 *Prog. Theor. Phys.* **16** 569
[11] Nikuni T, Oshikawa M, Oosawa A and Tanaka H 2000 *Phys. Rev. Lett.* **84** 5868
[12] Ruegg C, Cavadini N, Furrer A, Gudel H U, Kramer K, Mutka H, Habicht A K, Vorderwisch P and Wildes A 2003 *Nature* **423** 62
[13] Jaime M, Correa V F, Harrison N, Batista C D, Kawashima N, Kazuma Y, Jorge G A, Stern R, Heinmaa I, Zvyagin S A, Sasago Y and Uchinokura K 2004 *Phys. Rev. Lett.* **93** 087203
[14] Zapf V S, Zocco D, Hansen B R, Jaime M, Harrison N, Batista C D, Kenzelmann M, Niedermayer C, Lacerda A and Paduan A 2006 *Phys. Rev. Lett.* **96** 077204
[15] Andrianov S N and Moiseev S A 2014 *Phys. Rev. A* **90** 0423031
[16] Spek A L, Vaneijck B P, Jans R J F and Vankoten G 1987 *Acta Crystallogr. Sect. C-Cryst. Struct. Commun.* **43** 1878
[17] Busby R, Hursthouse M B, Jarrett P S, Lehmann C W, Malik K M A and Phillips C 1993 *J. Chem. Soc. Dalton.* 3767
[18] Oberhauser W, Bachmann C, Stampfl T, Haid R and Bruggeller P 1997 *Polyhedron* **16** 2827
[19] Davison J C, Foreman M R S, Howie R A, Plater M J and Skakle J M S 2001 *Acta Crystallogr. Sect. C-Cryst. Struct. Commun.* **57** 690
[20] Benial A M F, Ramakrishnan V and Murugesan R 2002 *Spectrochim Acta A* **58** 1703
[21] Gao W, Li K and Wang X L 2013 *Asian. J. Chem.* **25** 7876
[22] Pauling L 1936 *J. Chem. Phys.* **4** 673
[23] Lykos P G and Parr R G 1958 *J. Chem. Phys.* **28** 361
[24] Haberditzl W 1966 *Angew. Chem. Int. Edit.* **5** 288
[25] Honda Z, Asakawa H and Katsumata K 1998 *Phys. Rev. Lett.* **81** 2566
[26] Paduan A, Gratens X and Oliveira N F 2004 *Phys. Rev. B* **69** 0204051
[27] Blundell S 2009 *Magnetism in condensed matter* (Peking: Science Press) p. 93
[28] Salvador M, Gasparini N, Perea J D, Paleti H, Distler A, Inasaridze L N, Troshin P A, Luer L, Egelhaaf H J and Brabec C 2017 *Energy Environ. Sci.* **10** 2005
[29] Huang Y L, Yang R, Li P G and Xiao H 2020 *Chin. Phys. B* **29** 097405
[30] Tari A 2003 *The Specific Heat of Matter at Low Temperatures* (London:Imperial College Press) p. 150